International Journal of Microwave and Wireless Technologies

cambridge.org/mrf

A compact, dual-polarized patch antenna with improved T_X–R_X isolation for 2.4 GHz single frequency full-duplex applications

Haq Nawaz, Muhammad Abdul Basit and Ahmad Umar Niazi

Electronics Engineering, University of Engineering and Technology (UET) Taxila, Sub-Campus Chakwal, 48800 Chakwal, Pakistan

Research Paper

Cite this article: Nawaz H, Basit MA, Niazi AU (2021). A compact, dual-polarized patch antenna with improved T_x–R_x isolation for 2.4 GHz single frequency full-duplex applications. *International Journal of Microwave and Wireless Technologies* **13**, 266–273. https://doi.org/10.1017/S1759078720000537

Received: 4 February 2020
Revised: 14 April 2020
Accepted: 16 April 2020
First published online: 13 May 2020

Key words:
High interport isolation; full duplex antenna; differential feeding; dual polarization; self interference cancellation (SIC)

Author for correspondence:
Haq Nawaz,
E-mail: haq.nawaz@uettaxila.edu.pk

Abstract

A compact dual-polarized monostatic antenna (single radiator for transmit and receive modes) is presented with differential receive mode operation to achieve excellent interport isolation for 2.4 GHz single frequency full-duplex or in-band full-duplex applications. The presented antenna comprises three ports radiating element (patch) and a simple 3 dB/180° ring hybrid coupler has been utilized for differentially excited receive mode operation. The 3 dB/180° ring hybrid coupler acts as a self-interference cancellation (SIC) circuit for effective suppression of RF leakage from the transmit port to provide very high interport decoupling between transmit and receive ports. A compact antenna structure has been realized by using two-layered printed circuit board through vias interconnections of both receive ports of the antenna with inputs of SIC circuit. The validation model of proposed antenna offers more than 95 dB peak interport isolation. Moreover, the experimentally measured interport isolation is better than 70 dB throughout the antenna's 10 dB return-loss impedance bandwidth (BW) of 50 MHz (2.38–2.43 GHz). Furthermore, the recorded isolation is more than 80 dB in 20 MHz BW. The implemented antenna has good radiation characteristics including nice gain and low cross-polarization levels as endorsed by measurements. Same antenna structure with microstrip-T feeds can provide DC isolated ports with same interport RF isolation performance for active antenna applications. Such antenna with DC interport isolation will avoid the requirements of additional series capacitors on transmit and receive ports of antenna.

Introduction

In order to realize single frequency full-duplex (SFFD) also termed as in-band full-duplex (IBFD) wireless operation with its full gains, the IBFD transceiver should cancel the self-interference (SI) at the receiver side (which is induced by its own transmitter) to the receiver's noise floor [1–3]. Normally, the amount of suppressed SI is deemed as a figure of merit for SFFD radio transceiver design [2, 3]. The residual SI acts as a noise and decreases the signal to noise ratio which results in degradation to achievable throughput of full-duplex wireless operation [1]. The intended levels of SI suppression depend on the radiated power and bandwidth (BW) of transmitted signal in addition to received noise power (P_{rn}) at receiver. For example, the received noise power (P_{rn}) for the receiver with 20 MHz BW and 11 dB noise figure (NF) are computed as [3, 4]:

$$P_{\mathrm{rn}} = -174\,\mathrm{dBm} + 10\log(\mathrm{B.W}) + \mathrm{NF} \tag{1}$$

$$P_{\mathrm{rn}} = -174\,\mathrm{dBm} + 73 + 11 = -90\,\mathrm{dBm}$$

Based on (1) and as depicted in Fig. 1, if the transmitted power (P_t) for a radio transceiver is 10 dBm, then the required amount of SI suppression should be 10 dBm-(−90 dBm) = 100 dB so that received signal is not disturbed by RF leakage from its own transmitter (which is termed as SI in IBFD wireless communication context).

A large amount of SI suppression is required at the antenna stage to prevent the radio receiver to become saturate due to excessive SI [1–3, 5]. As depicted in Fig. 1, if we achieve around 70 dB SI suppression or SI cancellation (SIC) at antenna stage which is the case with our proposed antenna, then only 30 dB SIC using digital base-band techniques can achieve the total intended 100 dB isolation enabling the full-duplex operation at same transmit and receive carrier frequency without using complex and bulky analog RF domain SIC topologies. In addition, the non-linear components of SI (resulting from nonlinearities in T_x chain) and transmitter noise is also required to be suppressed [1, 4].

© Cambridge University Press and the European Microwave Association 2020

CAMBRIDGE UNIVERSITY PRESS

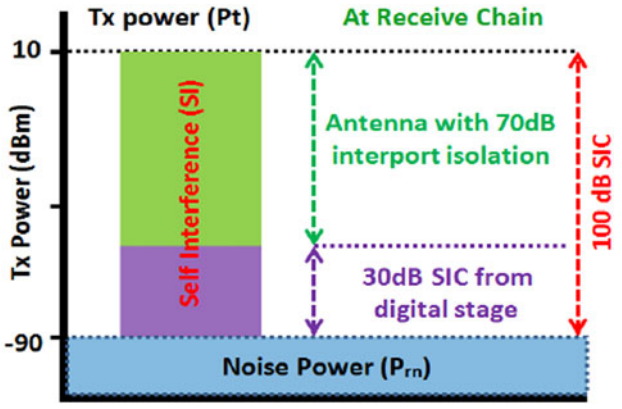


Fig. 1. Achieving around 100 dB self-interference cancellation (SIC) for an IBFD transceiver employing a monostatic antenna with 70 dB interport isolation.

The basic configuration of a dual-polarized, dual-port patch antenna is normally based on a square-shaped element with two perpendicular ports for excitation of vertical and horizontal polarizations for respective port excitation. Such dual-polarized antenna designed on 1.6 mm thick FR-4 substrate can offer ~30–35 dB T_x–R_x port–port isolation [5]. Moreover, hybrid feeding can be employed for such dual-polarized antennas to improve the interport isolation on the cost of additional complexity [5]. For instance, one such topology is reported in [5], where one port excites the patch through thin quarter-wave feed line and slot coupling is deployed for other polarization modes to achieve ~ 15–20 dB additional isolation. The microstrip-T can also be used instead of thin quarter-wave feed to achieve almost the same levels of interport isolation for such antennas with hybrid feeds [6]. The interport coupling can also be reduced through a defected ground structure as reported for an antenna presented in [7].

An external single or multi-taps SIC circuitry can be used with dual-port, dual-polarized antenna to suppress the T_x leakage at R_x port [8–11]. These SIC techniques are based on signal inversion mechanism where T_x signal is tapped and its modified version is subtracted from the coupled signal at R_x port. The achievable isolation levels with such techniques are highly dependent on the accuracy and resolution of active components in T_x signal modification channel. Moreover, such SIC topologies are inherently narrow-band and provide cancellation within very limited BW (few MHz) as detailed in [8, 9]. The two-taps circuitry can achieve comparatively wider SIC BW as reported for antennas in [10, 11].

Different excitation networks can also be used along with balanced circuitry to generate two orthogonal for T_x and R_x modes with reduced coupling and cross-polarization levels. However, such antenna designs are mostly based on the multi-layered printed circuit board (PCB) structures and complex balanced feed networks [12]. The SIC can also be performed through an extra signal path to achieve improved interport isolation. For example, the dual-port antenna reported in [13] is based on T_x leakage suppression through an additional signal path to obtain 20 dB interport isolation within 1.85–2.62 GHz frequency range. The cross-polarized antennas with improved interport isolation between DC isolated feeding ports are required for active integrated antenna topologies [14]. These types of antennas are also used for the implementation of retrodirective arrays [15] or amplifying-reflect arrays [16]. Previously reported antennas for such application have employed electromagnetic coupled (proximity feeding etc.)-based excitation or multilayered structures. The monostatic antennas with DC isolated ports will neither require DC blocking series capacitors at the output of T_x chain nor at the input of R_x port of radio transceiver. The dual-polarized antennas with high port–port isolation can effectively mitigate the fading effect for GSM and LTE bands mobile applications as discussed in [17]. The differential feeding is a very useful SIC technique to achieve high T_x–R_x isolation without degrading the radiation performance of monostatic antennas. The differential feeding can be used either at T_x/R_x or simultaneously at both ports [18–21]. The achievable SIC performance of differentially driven antennas is dependent upon the antennas symmetry and the response of the employed differential circuit. Moreover, the coupling between the radiating structure and differential circuit also limits the achievable isolation. The 3 dB/180° ring hybrid coupler with very nice amplitude and out-of-phase balance characteristics is a good choice for differential excitation of dual-polarized antennas to achieve high interport isolation.

The presented antenna topology is based on three ports patch with three symmetrically placed ports exciting the patch through thin quarter-wave (λ_g/4) feed lines. Two R_x ports are dual linear polarized with respect to a T_x port which results in the same amount of coupling for each pair of T_x–R_x ports. The differentially driven R_x mode through designated ports of antenna effectively suppresses the T_x leakage at R_x port through signal inversion mechanism without degradation in radiation characteristics of the antenna. The intended differential excitation is realized through a simple and well balanced 3 dB/180° ring hybrid coupler. The designed hybrid coupler has an excellent amplitude and out-of-phase balance response for the BW of interest (antenna's 10 dB return loss impedance BW). Consequently, the SI is well suppressed by the employed differential circuit within the intended range of frequencies. The theoretical analysis using simple circuit theory is also presented for employed SIC topology. The dependence of achievable SIC levels on amplitude and phase response of the differential circuit is analytically analyzed too. The validation model for the proposed antenna is realized with two-layered PCB. The patch with co-planar feeds is etched on the top of dielectric layer 1 and the differential circuit is implemented on bottom of dielectric layer 2 with shared ground plane sandwiched between two layers of substrate. The interconnections are made through small vias. This architecture results in compact antenna design and reduced PCB size. In addition, as compared to reported work in [18], this design achieves better interport isolation performance. The implemented antenna demonstrates ~10 dB additional isolation in 50 MHz BW compared to the reported antenna in [18]. The reason is that the achievable SIC performance is limited by strong coupling between the coupler and co-located radiating element for the antenna design reported in [18]. However, for stacked PCB design in current work, the patch and SIC circuit are electromagnetically isolated through the sandwiched ground plane. So here, the improvement in isolation is attributed to the reduced coupling between the patch and SIC circuit.

2.4 GHz Dual-polarized antenna with differentially driven R_x mode

The presented dual-polarized, 2.4 GHz antenna comprises three ports square patch antenna with quarter-wave (λ_g/4) feeds as shown in Fig. 2 below. The proposed antenna has been designed on 1.6 mm thick single-layered FR-4 substrate (ε_r = 4.4, tanδ = .02)

https://doi.org/10.1017/S1759078720000537 Published online by Cambridge University Press

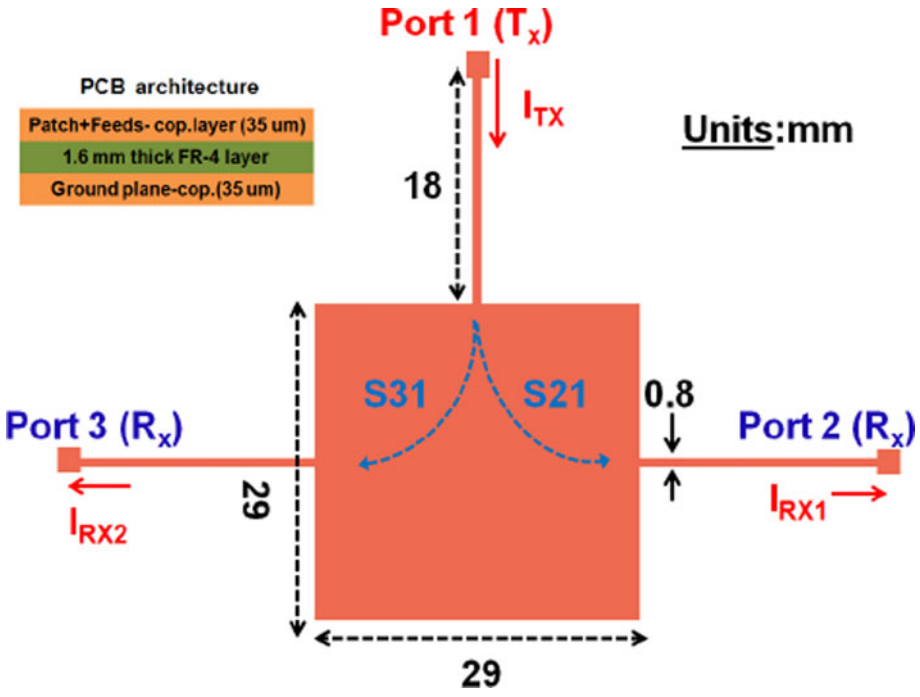


Fig. 2. Three ports microstrip patch antenna with a transmit port and pair of R_x ports which will be used for differential receive mode for self-interference suppression.

as indicated in Fig. 2. The port 1 is for transmit (T_x) mode while port 2 and port 3 will be used for differential-driven receive (R_x) mode. Due to the symmetry of the proposed antenna, the same amount of SI or RF power is leaked from T_x to each of R_x port.

Each R_x port is orthogonally linearly polarized with respect to T_x port (port 1) and as reported in [5], the interport isolation between each pair of T_x–R_x ports will be around 35 dB for such single-layered antenna designed on 1.6 mm thick FR-4 substrate. The differential excitation through R_x ports can suppress the T_x leakage to achieve additional isolation on the top of intrinsic isolation of polarization diversity as detailed through the following analysis. Let us denote I_{Rx1} and I_{Rx2} as currents flowing out of R_x ports and they are related with input current I_{Tx} (current flowing in to T_x port) through following equations:

$$I_{Rx1} = I_{Tx}\, S_{21} \text{ and } I_{Rx2} = I_{Tx}\, S_{31}, \tag{2}$$

where S_{21} and S_{31} are the magnitudes of coupling co-efficients for respective pair of T_x–R_x ports.

With the differentially driven R_x port, the total current I_{Rx} flowing out will be given as:

$$I_{Rx} = \frac{1}{\sqrt{2}}(\, e^{j180^\circ} I_{Rx1} + I_{Rx2}) = \frac{I_{Tx}}{\sqrt{2}}(\, S_{31} - S_{21}). \tag{3}$$

Based on (3), the interport current coupling and isolation transfer functions are given as:

$$\frac{I_{Rx}}{I_{Tx}} = \frac{1}{\sqrt{2}}\,(\, S_{31} - S_{21}), \tag{4}$$

$$\frac{I_{Tx}}{I_{Rx}} = \frac{\sqrt{2}}{(\, S_{31} - S_{21})}. \tag{5}$$

As stated earlier, based on the symmetry of the proposed antenna, the same amount of SI or RF power results from T_x to each of R_x port. For perfect or ideal symmetrical structure $S_{21} = S_{31}$.This will result in perfect cancellation of SI at R_x port to provide infinite interport isolation based on (5) if an ideal differential circuit is employed. However, in reality for a carefully designed antenna $S_{21} \approx S_{31}$, excellent SIC levels can be obtained when a differential circuit with nice amplitude and phase balance characteristics is employed with proposed three ports antenna and both are electromagnetically isolated.

The dependence of achievable SIC levels on the amplitude and an out-of-phase imbalance of differential circuit is analyzed graphically as illustrated in Fig. 3. The plot in Fig. 3 provides the difference (in dB) between two same frequency AC signals with different magnitude and phase values. The magnitude and phase difference between two signals is termed as magnitude and phase errors of the differential feeding network (DFN). As expected and stated earlier, the difference (in dB) or SIC levels are highly dependent on both magnitude and phase errors as clear from Fig. 3. For instance, the SIC levels are reduced from 45 dB to around 37 dB for two out-of-phase signals with 0.1 dB magnitude error. Similarly, the SIC levels are reduced from 35 dB to 30 dB for the case of 0.1 dB and 1° phase errors, respectively. However, as indicated in Fig. 3, SIC levels between 30 dB and 45 dB can be achieved through a differential circuit with magnitude error $\leq$ 0.3 dB and phase error $\leq$ 1°.

The simulated return loss and port–port isolation results for proposed three ports antenna depicted in Fig. 2 are presented in Fig. 4. The three ports antenna was simulated by using Ansoft HFSS13 software. The reference impedance for each port was set to 50Ω for these simulations. As clear from Fig. 4, the ideal differential feeding circuit (having zero magnitudes, phase errors) can provide around 80 dB interport isolation within 10 dB return loss BW of 50 MHz. The simulated peak isolation exceeds 100 dB in this case. So more than 50 dB isolation is provided through differential feeding-based SIC operation on top of 30–35 polarization diversity isolation for 50 MHz BW. The asymmetric behavior of interport isolation is due to low mesh density

https://doi.org/10.1017/S1759078720000537 Published online by Cambridge University Press

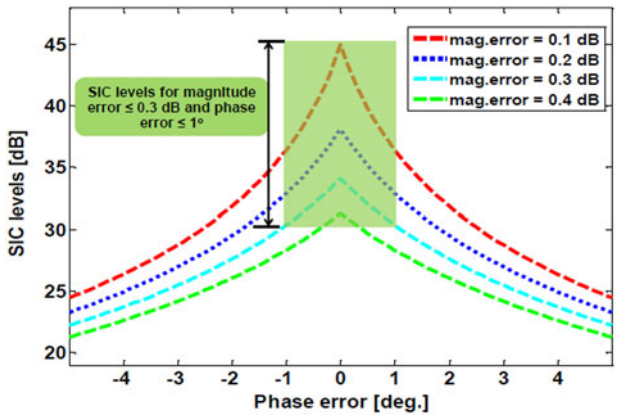


Fig. 3. The illustration of SIC levels dependence on magnitude and phase error of DFN.

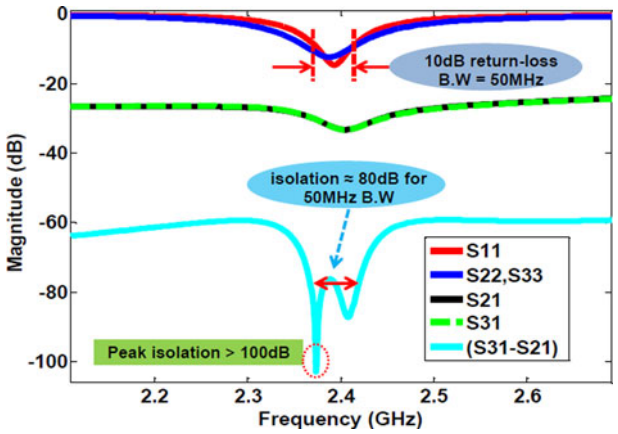


Fig. 4. The simulated *S*-parameters for three ports antenna with one T_x port and two R_x ports.

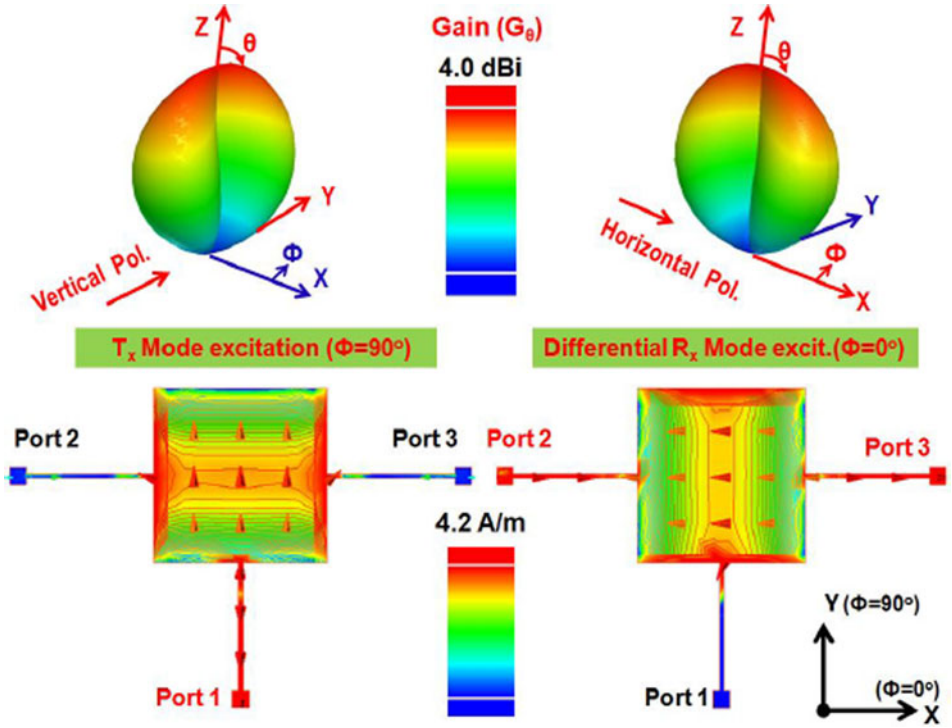


Fig. 5. The simulated surface current distributions and 3D radiation patterns for T_x mode and differential R_x mode of three ports antenna for respective port excitation at $f = 2.4$ GHz.

which was used to save the computational resources and reduce the simulation times.

The simulated dual-polarized characteristics of the presented three ports antenna with differential R_x mode are presented in Fig. 5. As clear from simulated surface currents distribution and gain patterns in Fig. 5, the antenna resonates at the same frequency of 2.4 GHz with vertical and horizontal polarization for T_x and differential-fed R_x modes, respectively. The differentially excited R_x mode also achieves reduced cross-polarization levels through the cancellation of higher-order modes and enables the patch to operate with TM_{01} and TM_{10} modes (fundamental modes of square-shaped radiating patch) only as detailed in [22].

A 2.4 GHz, 3 dB/180° ring hybrid coupler has been used for required differential excitation at R_x port. The coupler is used as 3 dB out-of-phase power divider. The hybrid coupler acts as SIC circuit to perform (S_{31}–S_{21}) operation when it is connected with three ports antenna and its difference port (Δ port) is used as R_x port. The simulated hybrid coupler achieves excellent amplitude and out-of-phase balance response for BW of interest (antenna's 10 dB return loss impedance BW). Consequently, the SI is well suppressed by the employed differential circuit (hybrid coupler) with an intended range of frequencies. The design details and simulated results of 3 dB/180° ring hybrid coupler are not presented here for brevity.

Antenna prototype and measurement results

The physical model or prototype of the miniaturized dual port, dual-polarized monostatic IBFD antenna with differentially driven R_x mode is shown in Fig. 6. The overall dimensions of the implemented antenna are 75mm × 70 mm as shown in Fig. 6. The validation model was realized by using double-layered FR-4

https://doi.org/10.1017/S1759078720000537 Published online by Cambridge University Press

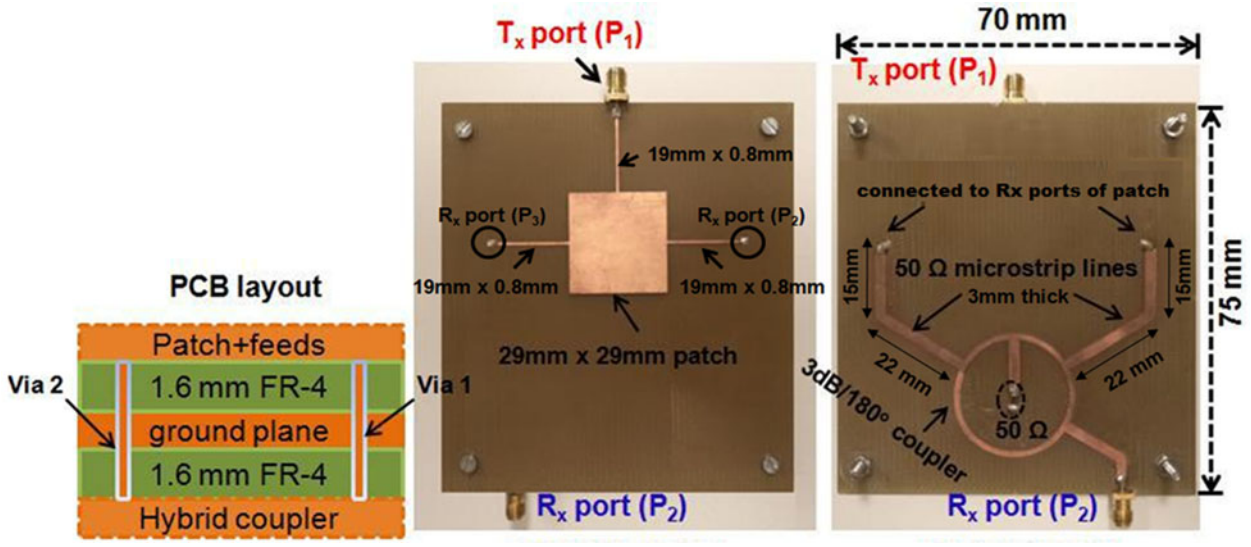


Fig. 6. The physical model of 2.4 GHz differential fed IBFD monostatic antenna.

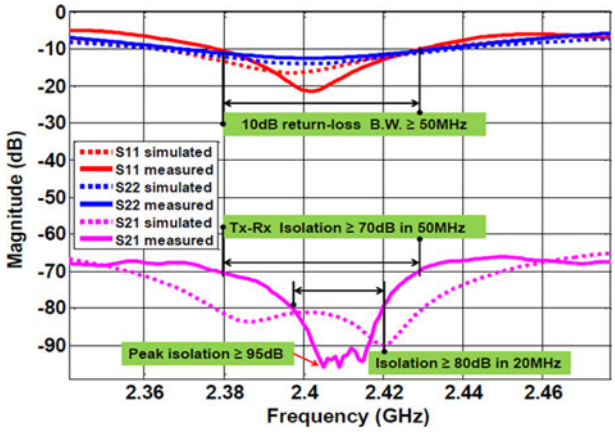


Fig. 7. The simulated and measured *S*-parameters (S_{11}, S_{22}, S_{21}) for IBFD antenna.

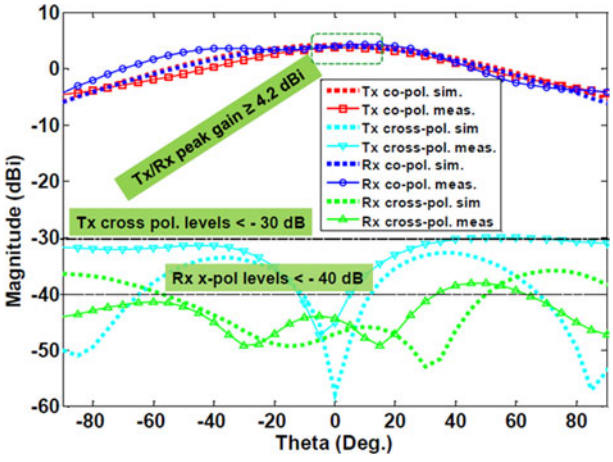


Fig. 8. The simulated and measured co-polarization and cross-polarization gain patterns for presented monostatic IBFD antenna at 2.4 GHz frequency band.

($\varepsilon_r = 4.4$, $\tan\delta = .02$) dielectric with 1.6 mm thickness of each layer. The three ports patch was etched on top of FR-4 layer 1 while hybrid coupler was placed on the lower side of FR-4 layer 2 as indicated in Fig. 6. The ground plane is placed between two layers of FR-4 substrate. The interconnections are made through small vias. This results in compact antenna design and reduced PCB size. The implemented antenna can be directly connected to single-in single-out transceiver through designated T_x and R_x ports. The T_x and R_x ports of the implemented antenna can be interchanged without degradation in antenna's interport isolation performance. However, the ports of IBFD antenna on a second wireless node should also be interchanged to align the intended polarization of forward and reverse links of dual-polarized full-duplex channel as discussed in [20, 23].

The performance of the implemented antenna has been characterized through *S*-parameters and gain measurements for each polarization. The recorded results for S_{11}, S_{22}, and T_x–R_x interport coupling (S_{21}) for validation model are presented in Fig. 7. The simulation *S*-parameters were obtained through Keysight ADS software. The three ports antenna was simulated by using Ansoft HFSS13 software. The 3 dB/180° ring hybrid coupler was simulated in Keysight ADS Momentum software with mesh density = 20 cells/wavelength. The *S*-parameters for the three ports antenna were imported from HFSS to ADS. Then, the imported *S*-parameters and EM model of coupler were used in ADS schematic to obtain the simulated *S*-parameters (S_{11}, S_{22}, S_{21}) for the compact antenna structure.

The physical model or the prototype achieves the shared 10 dB return- loss impedance BW of 50 MHz (2.38–2.43 GHz) for each of T_x and R_x port. The physical model achieves ≥ 70 dB isolation (negative of measured T_x–R_x interport coupling) throughout the 50 MHz BW (spans over 2.38–2.43 GHz). Moreover, the measured peak isolation exceeds 95 dB peak near 2.41 GHz as marked in Fig. 7. Furthermore, better than 80 dB isolation has been observed for the frequency span of 2.4–2.42 GHz (20 MHz BW). Consequently, for 50 MHz BW ~45 dB isolation is contributed by SIC circuit on the top of polarization isolation. The difference between the simulated and measured results can be attributed to the fabrication inaccuracies and the soldering imperfections.

https://doi.org/10.1017/S1759078720000537 Published online by Cambridge University Press

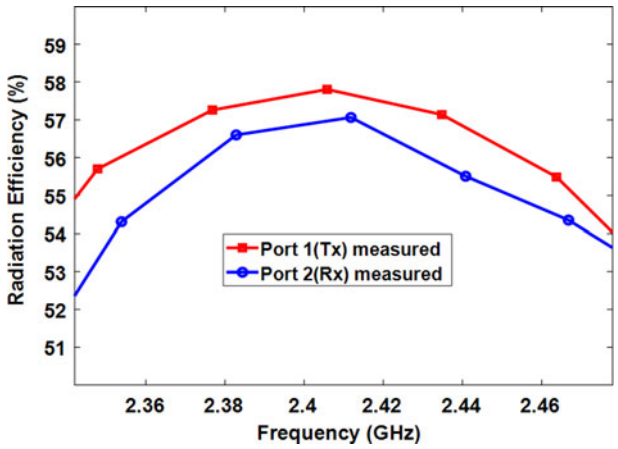


Fig. 9. The measured radiation efficiencies for the presented antenna when respective T_x and R_x port are excited with other ports terminated in 50 Ω loads.

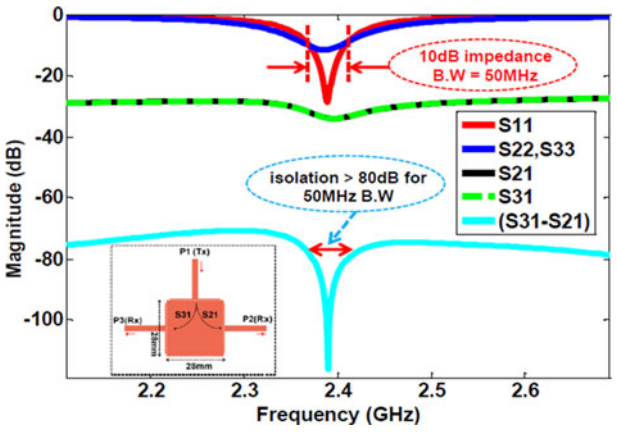


Fig. 10. Simulated port matching (S_{11}, S_{22}) and interport isolation (S_{12}) for three ports patch antenna with microstrip-T feeds to achieve DC interport isolation.

Table 1. The performance comparison of the presented antenna with other monostatic antennas which were reported earlier in [12, 18, 20, 23, 24, 26]

Ref. antennas	Peak isolation	10 dB return loss B.W.	Isolation versus SIC B.W.	Antenna Size (mm^3)	Substrate/PCB layers	Peak rad. efficiency
[12]	34 dB	19%	28 dB for 410 MHz	100 × 43 × 9.2	0.8 mm FR-4/three layers	Not given
[18]-Antenna1	67 dB	50 MHz	62 dB for 50 MHz	110 × 90 × 1.6	1.6 mm FR-4/single layer	50%
[18]-Antenna2	90 dB	50 MHz	70 dB for 50 MHz	120 × 90 × 3.2	1.6 mm FR-4/double layer	50%
[20]	98 dB	50 MHz	80 dB for 40 MHz	125 × 84 × 1.6	1.6 mm FR-4/double layer	57%
[23]	78 dB	50 MHz	64 dB for 50 MHz	105 × 88 × 1.6	1.6 mm FR-4/single layer	50%
[26]	≥55 dB	250 MHz	40 dB for 250 MHz	Not given	0.81 mm thick R04003C	Not given
[24]	95 dB	45 MHz	85 dB for 45 MHz	100 × 95 × 3.2	1.6 mm FR-4/double layer	55%
This design	≥95 dB	50 MHz	70 dB for 50 MHz 80 dB for 20 MHz	75 × 70 × 3.2	1.6 mm FR-4/double layer	≥56%

The simulated and experimentally recorded co-polarized and cross-polarized gain patterns for implemented dual port, dual-polarized monostatic IBFD antenna are also recorded and presented in Fig. 8. These patterns have been measured at 2.4 GHz frequency band for both T_x and R_x modes, respectively. The measured gain is better than 4.2 dBi for each of T_x and R_x port as clear from Fig. 8. Moreover, the recorded cross-polarization levels for the prototype are more than 30 and 40 dB below the respective co-polarized levels. Thus, the antenna offers nice gain levels with excellent polarization purity in addition to highly decoupled T_x–R_x ports for IBFD applications.

The measured radiation efficiencies for the presented antenna are given in Fig. 9 for respective T_x and R_x ports excitations with other ports terminated in 50Ω loads. These results were measured through EMSCAN RFxpert near-field measurement configuration for the respective ports. The recorded peak radiation efficiencies are better than 56% for both T_x and R_x ports as clear from Fig. 9. The low radiation efficiencies for the presented antenna are due to the high loss (loss tangent) of FR-4 substrate which was used for antenna implementation. The radiation efficiencies and the resulting gains for T_x and R_x modes of the presented antenna can be improved significantly by using low loss dielectric/substrate as detailed in [20, 23, 24].

Dual-polarized antenna with high RF isolation between the DC isolated ports

By replacing the thin $\lambda_g/4$ feeds with microstrip-T (MS-T) feeds for the presented antenna, the DC isolation between T_x and R_x ports can be achieved in addition to high RF interport isolation [23, 25]. Such MS-T feeds excite the antenna through EM coupling and antenna can be effectively used for active applications where DC interport isolation is required [14–16]. The simulated *S*-parameters results for three-port antenna with MS-T feeds are shown in Fig. 10. The proposed antenna achieves around 120 dB peak interport isolation and more than 80 dB port to port isolation

https://doi.org/10.1017/S1759078720000537 Published online by Cambridge University Press

for 50 MHz BW as clearly depicted in Fig. 10. The differential feeding can be used for this antenna for R_x mode to achieve high interport isolation between DC isolated ports as presented in [23]. The isolation can be further improved through stacked PCB structure where patch and SIC will be electromagnetically isolated through the ground plane as was the case for antenna presented in previous sections. In that case, the PCB size will also be reduced compared to the antenna design reported in [23].

The dimensions and experimentally characterized interport isolation performance of the presented antenna are compared with other monostatic antennas which were reported earlier in [12, 18, 20, 23, 24, 26]. This comparison is detailed in Table 1 which provides the peak isolation, 10 dB return-loss BW, amount of SIC versus SIC BW, dimensions, type of substrate, number of substrate layers, and peak radiation efficiencies for various prototypes of IBFD monostatic antennas. As clear from Table 1, the validation model of our proposed, dual-polarized monostatic IBFD antenna is more compact as compared to previously reported monostatic antennas. The dimensions of the presented antenna are only $(0.6 \times 0.55 \times 0.03)\ \lambda_o$ where λ_o is the free space wavelength for 2.4 GHz frequency. The validation model of proposed antenna also offers comparatively better performance in terms of interport isolation versus SIC BW along with very high levels of peak isolation as obvious from Table 1. These enhanced levels of interport isolation for presented compact antenna structure are attributed to effective SIC performed through differential feeding circuit. Moreover, these SIC improvements stem from the electromagnetic isolation (through intermediate ground plane) of monostatic antenna element and associated differential feeding circuit. This electromagnetic isolation offers reduced interport coupling (around 10 dB reduction) as compared to differentially driven antennas reported in [18, 20, 23].

Conclusion

A high isolation, compact (75 mm × 70 mm), two-port, dual-polarized, monostatic patch antenna has been presented here for 2.4 GHz IBFD applications. The proposed antenna employs differential feeding at R_x port to achieve high interport isolation. The differential excitation is achieved through a simple and well balanced 3 dB/180° ring hybrid coupler. The deployed hybrid coupler has an excellent amplitude and out-of-phase balance response for the BW of interest and SI is well suppressed by the employed differential circuit within 10 dB return loss impedance BW of antenna. The DFN provides 45–50 dB additional isolation which is superimposed on 30–35 dB polarization diversity isolation. The electromagnetic isolation between the monostatic radiating element and SIC provides ~10 dB improvement in isolation along with reduced PCB size compared to previously reported design based on the same topology. The physical model with 80 dB T_x–R_x isolation within 20 MHz BW can be deployed for low power IBFD wireless link without additional RF domain SIC techniques or stages.

References

1. **Bharadia D, McMilin E and Katti S** (2013) Full Duplex Radios. ACM SIGCOMM 2013, Hong Kong.
2. **Maraševic J, Zhou J, Krishnaswamy H, Zhong Y and Zussman G** (2017) Resource allocation and rate gains in practical full-duplex systems. *IEEE/ACM Transactions on Networking* **25**, 292–305.
3. **Korpi D, *et al.*** (2014) Full-duplex transceiver system calculations: analysis of ADC and linearity challenges. *IEEE Transactions on Wireless Communications* **13**, 3821–3836.
4. **Anttila L, Korpi D, Syrjälä V, *et al.*** (2013) Cancellation of power amplifier induced nonlinear self-interference in full-duplex transceivers. *2013 Asilomar Conference on Signals, Systems and Computers, Pacific Grove, CA*, pp. 1193–1198.
5. **Nawaz H and Tekin I** (2016) Three dual polarized 2.4 GHz microstrip patch antennas for active antenna and in-band full duplex applications. *2016 16th Mediterranean Microwave Symposium (MMS), Abu Dhabi, United Arab Emirates*, pp. 1–4. doi: 10.1109/MMS.2016.7803854.
6. **Amjad MS, Nawaz H, Özsoy K, Gürbüz Ö and Tekin I** (2018) A low-complexity full-duplex radio implementation with a single antenna. *IEEE Transactions on Vehicular Technology* **67**, 2206–2218.
7. **Younkyu C, Seong-Sik J, Ahn D, *et al.*** (2004) High isolation dual-polarized patch antenna using integrated defected ground structure. *IEEE Microwave and Wireless Components Letters* **14**, 4–6.
8. **Nawaz H and Tekin I** (2016) Dual port single patch antenna with high interport isolation for 2.4 GHz in-band full duplex wireless applications. *Microwave and Optical Technology Letters* **58**, 1756–1759.
9. **Nawaz H, Gürbüz Ö and Tekin I** (2018) High isolation slot coupled antenna with integrated tunable self interference cancellation (SIC) Circuitry. *Electronics Letters* **54**, 1311–1312.
10. **Kolodziej K, McMichael J and Perry B** (2016) Multitap RF canceller for In-band full-duplex wireless communications. *IEEE Transactions on Wireless Communications* **15**, 4321–4334.
11. **Nawaz H, Gürbüz Ö and Tekin I** (2019) 2.4 GHz Dual polarized monostatic antenna with simple two-taps RF Self Interference Cancellation (RF-SIC) circuitry. *Electronics Letters* **55**, 299–300.
12. **Deng C, Li Y, Zhang Z, *et al.*** (2014) A wideband high-isolated dual-polarized patch antenna using two different balun feedings. *IEEE Antennas and Wireless Propagation Letters* **13**, 1617–1619.
13. **Zhang Y and Wang P** (2016) Single ring two-port MIMO antenna for LTE applications. *Electronics Letters* **52**, 998–1000.
14. **Chang K, York RA, Hall PS and Itoh T** (2002) Active integrated antennas. *IEEE Transactions on Microwave Theory and Techniques* **50**, 937–944.
15. **Luxey C and Laheurte J-M** (1999) A retrodirective transponder with polarization duplexing for dedicated short range communications. *IEEE Transactions on Microwave Theory and Techniques* **47**, 1910–1915.
16. **Bialkowski ME and Song HJ** (2002) Investigation into a power-combining using a reflect-array of dual polarized aperture-coupled microstrip patch antennas. *IEEE Transactions on Antennas and Propagation* **50**, 841–849.
17. **Puente C, Anguera J and Borja C** (2005) Dual-band dual-polarized antenna array. US Pat. 6,937,206.
18. **Nawaz H and Tekin I** (2017) Dual-polarized, differential fed microstrip patch antennas with very high interport isolation for full-duplex communication. *IEEE Transactions on Antennas and Propagation* **65**, 7355–7360.
19. **Yilan M, Ayar H, Nawaz H, Gurbuz O and Tekin I** (2019) Monostatic antenna In-band full duplex radio: performance limits and characterization. *IEEE Transactions on Vehicular Technology* **68**, 4786–4799.
20. **Nawaz H and Tekin I** (2018) Double differential fed, dual polarized patch antenna with 90 dB interport RF isolation for 2.4 GHz In-band full duplex transceiver. *IEEE Antennas and Wireless Propagation Letters* **17**, 287–290.
21. **Nawaz H and Umar Niazi A** (2019) A compact proximity-fed 2.4 GHz monostatic antenna with wide-band SIC characteristics for in-band full duplex applications. *International Journal of RF and Microwave Computer-Aided Engineering* **30**, e22087.
22. **Liang X-L, Zhong S-S and Wang W** (2005) Design of a dual-polarized microstrip patch antenna with excellent polarization purity. *Microwave and Optical Technology Letters* **44**, 329–331.
23. **Nawaz H and Basit A** (2019) Single layer, dual polarized, 2.4 GHz patch antenna with very high RF isolation between DC isolated T_x–R_x ports for full duplex radio. *Progress In Electromagnetics Research Letters* **85**, 65–72.
24. **Nawaz H, Basit MA and Shaukat F** (2020) Dual polarized, slot coupled monostatic antenna with high isolation for 2.4 GHz full duplex applications. *Microwave and Optical Technology Letters* **62**, 1291–1298.

https://doi.org/10.1017/S1759078720000537 Published online by Cambridge University Press

25. **Kurup DG, Rydberg A and Himdi M** (2002) Compact microstrip-T coupled patch antenna for dual polarisation and active antenna applications. *Electronics Letters* **38**, 1240–1241.
26. **Khaledian S, Farzami F, Smida B and Erricolo D** (2018) Inherent self-interference cancellation for In-band full-duplex single-antenna systems. *IEEE Transactions on Microwave Theory and Techniques* **66**, 2842–2850.



Haq Nawaz received the B.Sc. degree in electrical engineering and the Master's degree in telecommunication engineering from the University of Engineering and Technology (UET), Taxila, Pakistan, in 2005 and 2012, respectively. He received the Ph.D. degree in Electronic Engineering from Sabanci University, Istanbul, Turkey. From January 2017 to June 2018, he has worked as post-doc research fellow with Faculty of Engineering and Natural Sciences (FENS), Sabanci University, Turkey. During 2006–2009, he was with SUPARCO Pakistan as a RF Design Engineer. He served UET Taxila, Sub-campus Chakwal, Pakistan, as a Lecturer in Electronics Engineering from 2010 to 2012.

Currently, he is working as Assistant Professor at Department of Electronics Engineering, UET Taxila, Sub-campus Chakwal, Pakistan. His research interests include full-duplex antenna design, RF circuits design and measurements for Radar and Satellite systems, beam-switched and phased scanning array antennas design and indoor positioning systems design.



Muhammad Abdul Basit received the B.S. degree in telecommunication engineering from FAST NUCES Islamabad, the M.S. degree in electrical engineering from UET Taxila, and the Ph.D. degree in communication and information engineering from the University of Electronic Science and Technology of China (UESTC), in 2016.

He has been an Assistant Professor with the Department of Electronics Engineering, UET Taxila, Sub-Campus Chakwal, since 2007. His area of specialization in the Ph.D. was antenna design. His research interests include flush-mounted antenna design, dual-polarized antenna design, and phased scanning array antennas.



Ahmad Umar Niazi received the B.Sc. degree in electrical engineering with specialization in communication & electronics from the University of Engineering & Technology (UET), Lahore, Pakistan and the Master's degree in electrical engineering from the University of Engineering and Technology (UET), Taxila, Pakistan, in 2001 and 2012, respectively. He is now pursuing his Ph.D. degree in electrical engineering from UET Taxila, Pakistan. He served at private and public sector industries/organizations from 2001 to 2006. He joined UET Taxila, Sub-campus Chakwal, Pakistan, and served as a lecturer in electronics engineering from 2007 to 2012.

Since 2012, he is working as Assistant Professor at Department of Electronics Engineering, UET Taxila, Sub-campus Chakwal, Pakistan. His research interests include microwave antenna design, antennas for 5 G applications, full-duplex antenna design, RF circuits design, beam-switched and phased scanning array antennas, and multi-band jamming techniques.

https://doi.org/10.1017/S1759078720000537 Published online by Cambridge University Press